Heat and matter transport in binary liquid mixtures

David MacGowan* and Denis J. Evans
Research School of Chemistry, Australian National University, G.P.O. Box 4, Canberra, Australian Capital Territory 2601, Australia
(Received 28 January 1986)

Following some preliminary clarification of microscopic heat current definitions for mixtures, we describe nonequilibrium molecular dynamics algorithms for the evaluation of heat and matter transport coefficients in binary liquid mixtures. Simulations have been carried out for a dense fluid of Lennard-Jones atoms, approximating an equimolar argon-krypton mixture, at a thermodynamic state which has been studied in several previous equilibrium simulations. Our results suggest that the estimates of the mutual diffusion coefficient from these equilibrium simulations are ~15% too high. Most importantly, we determine the cross-coupling coefficients which characterize the Soret and Dufour effects. These are obtained from two entirely independent sets of simulations and are found to be equal, in accordance with an Onsager reciprocal relation. When we run our algorithms with high external fields, we incidentally find evidence of demixing which is of interest in the general context of nonequilibrium phase transitions.

I. INTRODUCTION

Accurate kinetic theories for dense fluids are lacking and, as a result, most of our knowledge of liquid transport coefficients comes from computer simulations. The earliest methods using equilibrium molecular dynamics and Green-Kubo relations have now been largely superseded by nonequilibrium molecular dynamics[1] (NEMD) where the current caused by an applied external force is measured. Early boundary driven NEMD algorithms (with the exception of Lees-Edwards homogeneous shear[2]) suffered from incompatibility with periodic boundary conditions leading to results that were strongly dependent on system size. This problem has been overcome by the recent development of synthetic homogeneous NEMD algorithms so that it is now possible to obtain transport coefficients by simulating systems as small as those used in simulations of equilibrium properties, although it must be admitted that the run times have to be much greater than for equilibrium thermodynamic properties.

The work of the present paper is most directly based on the "color current" self-diffusion algorithm of Evans *et al.*[3] and the thermal conductivity algorithm of Evans,[4] which has since been used in other publications.[5–7] We give the generalizations of these algorithms to binary mixtures in Sec. III. This is quite straightforward once the appropriate microscopic definition of the heat current is identified. We discuss this point in some detail in Sec. II since the noninstantaneous character of the definitions in the existing literature makes them inconvenient for simulations. The numerical results for a single state point of an argon-krypton mixture are discussed in Sec. IV, followed by concluding remarks in Sec. V. The major contribution of the present paper is that it provides the first determination by any simulation method of a thermal diffusion ratio in a binary mixture. (Gillan and Holloway[8] have simulated the heat of transport for a model of defect motion in a one-dimensional solid, which is somewhat analogous.)

II. FORMALISM

A. Macroscopic

All of the results quoted in this section are standard and can be found in many textbooks, for example.[9–11(a)] The reason for this brief review of the macroscopic results is partly to fix notations but also an attempt to make as clear as possible the differences of the present work from previous microscopic treatments of transport in mixtures.

In the absence of external forces and chemical reactions, the (hydrodynamic) equations of matter, momentum, and energy transport take the form

$$\rho\frac{dx_\nu}{dt}=-\nabla\cdot\mathbf{J}_\nu\,, \tag{1}$$

$$\rho\frac{d\mathbf{u}}{dt}=-\nabla\cdot\underline{P}\,, \tag{2}$$

$$\rho\frac{de}{dt}=-\nabla\cdot\mathbf{J}'_Q-\nabla\mathbf{u}:\underline{P}\,, \tag{3}$$

where ρ is the total mass density, x_ν is the mass fraction of species ν, $\mathbf{u}$ is the barycentric velocity, $\underline{P}$ is the pressure tensor, and e is the specific internal energy. In addition, $\mathbf{J}_\nu=x_\nu\rho(\mathbf{u}_\nu-\mathbf{u})$ is the diffusion current density of species ν with center-of-mass velocity $\mathbf{u}_\nu$, and $\mathbf{J}'_Q$ is the total energy current density excluding convection and viscous dissipation. We also have, for entropy transport,

$$\rho\frac{ds}{dt}=-\nabla\cdot\mathbf{J}_s+\delta\,, \tag{4}$$

where s is the specific entropy, $\mathbf{J}_s$ is the entropy current density excluding convection, and δ is the entropy source strength per unit volume and unit time.

Assuming local thermodynamic equilibrium,

$$T\frac{ds}{dt}=\frac{de}{dt}-\frac{p}{\rho^2}\frac{d\rho}{dt}-\sum_\nu \mu_\nu\frac{dx_\nu}{dt}\ , \tag{5}$$

where p is the pressure and μ_ν the specific chemical potential of species ν, we can substitute Eqs. (1)—(3) in Eq. (5) and hence make the identifications

$$\mathbf{J}_s=\frac{1}{T}\left[\mathbf{J}'_Q-\sum_\nu \mu_\nu\mathbf{J}_\nu\right]\ , \tag{6}$$

$$\delta=-\frac{1}{T^2}\mathbf{J}'_Q\cdot\nabla T-\frac{1}{T}\sum_\nu \mathbf{J}_\nu\cdot[T\nabla(\mu_\nu/T)]-\frac{1}{T}\underline{\Pi}:\nabla\mathbf{u}\ , \tag{7}$$

where $\underline{\Pi}=\underline{P}-\frac{1}{3}p\underline{1}$.

$\mathbf{J}'_Q$ is the heat flow measured experimentally, but for theoretical purposes it is much more convenient to define

$$\mathbf{J}_Q=\mathbf{J}'_Q-\sum_\nu h_\nu\mathbf{J}_\nu\ , \tag{8}$$

where h_ν is the specific enthalpy of species ν. Now we can write

$$\delta=-\frac{1}{T^2}\mathbf{J}_Q\cdot\nabla T-\frac{1}{T}\sum_\nu \mathbf{J}_\nu\cdot\nabla_T\mu_\nu-\frac{1}{T}\underline{\Pi}:\nabla\mathbf{u}\ . \tag{9}$$

with the definition $\nabla_T\mu_\nu=\nabla\mu_\nu-(\partial\mu_\nu/\partial T)\nabla T$. This transformation removes from $\mathbf{J}'_Q$ the heat-flux contribution associated with interdiffusion of one species through the others and removes from the diffusive driving force (chemical potential gradient) that part caused purely by the temperature gradient.

Identifying the forces and fluxes in Eq. (9) and specializing to the case of a binary mixture we obtain, noting that $\mathbf{J}_2=-\mathbf{J}_1$, the following form of the phenomenological linear laws:

$$\mathbf{J}_1=L_{11}\mathbf{X}_1+L_{1Q}\mathbf{X}_Q\ , \tag{10}$$

$$\mathbf{J}_Q=L_{Q1}\mathbf{X}_1+L_{QQ}\mathbf{X}_Q\ , \tag{11}$$

where

$$\mathbf{X}_1=-\frac{1}{T}\nabla_T(\mu_1-\mu_2)\ , \tag{12}$$

$$\mathbf{X}_Q=-\frac{1}{T^2}\nabla T\ . \tag{13}$$

We ignore the laws describing viscous dissipation since, by Curie's principle, they do not couple to the heat and matter transport in the linear regime. The phenomenological cross coefficients L_{1Q} and L_{Q1} describe thermal diffusion (the Soret effect) and the diffusion thermoeffect (Dufour effect), respectively. According to an Onsager reciprocal relation (ORR),

$$L_{Q1}=L_{1Q}\ . \tag{14}$$

For completeness, we shall now give the relations between the L_{ab} and the transport coefficients which are most directly accessible experimentally. In subsequent sections, however, we shall only give results for the L_{ab}.

If we write Fick's Law for isothermal diffusion in the form

$$-\mathbf{J}_1=\rho D_1\nabla x_1\ , \tag{15}$$

then we obtain, using the Gibbs-Duhem relation,

$$D_1=\frac{L_{11}\partial\mu_1/\partial x_1}{\rho x_2 T}\ . \tag{16}$$

Here D_1 is the bulk diffusion coefficient of species 1 relative to the local center of mass. This means that, for unequal mass species, the diffusion is measured with respect to a moving plane. Experimentally the diffusion current is measured relative to the local center of volume and the relevant diffusion coefficient is then

$$D=\rho v_2 D_1\ , \tag{17}$$

where v_2 is the partial specific volume of species 2. As implied by our notation, D has the advantage over D_1 of being the same for both species. There is a multitude of other possible definitions of diffusion coefficient,[9,10,12] but we ignore these and refer to D as *the* mutual diffusion coefficient.

Measurements of the Soret effect are generally carried out in the steady state defined by $\mathbf{J}_1=0$. There are various coefficients that have been used to quantify the phenomenon. From these we arbitrarily choose the thermal diffusion ratio k_T, defined by

$$T\nabla x_1=-k_T\nabla T\ . \tag{18}$$

From Eqs. (10) and (15) it is easily seen that

$$k_T=\frac{L_{1Q}}{\rho T D_1}\ . \tag{19}$$

The Dufour effect, though easily seen in gases, is hard to measure accurately for liquids. An experimental value for L_{Q1} can be deduced from L_{1Q} and the ORR (14).

Fourier's law of heat conduction is, in the form applicable to most experimental determinations for mixtures,

$$-\mathbf{J}'_Q=\lambda\nabla T\ . \tag{20}$$

Again measurements are most commonly made in the steady state $\mathbf{J}_1=0$. Noting that, for the steady state, $\mathbf{J}'_Q=\mathbf{J}_Q$ and using Eqs. (10), (11), and (14) it is found that

$$\lambda=\frac{1}{T^2}\left[L_{QQ}-\frac{L_{1Q}^2}{L_{11}}\right]\ . \tag{21}$$

Even the (more difficult) experimental measurement of heat current in the uniform state $\mathbf{X}_1=0$ is not sufficient to determine L_{QQ} itself, since then $\mathbf{J}'_Q\neq\mathbf{J}_Q$.

B. Microscopic

We consider a system of N particles, N_1 of mass m_1 and N_2 of mass m_2, contained in a box of volume V. For brevity we adopt the notation that $\sum$ represents a sum over all particles and $\sum^\nu$ represents a sum only over particles of species ν. It is implicitly assumed that in double sums the two indices are not permitted to be equal. $\mathbf{q}_i$ and $\mathbf{p}_i$ denote the position and momentum, respectively, of particle i and $\mathbf{q}_{ij}=\mathbf{q}_j-\mathbf{q}_i$. The interaction energy of

the pair (i,j) is ϕ_{ij} and the force on i due to j is $\mathbf{F}_{ij}$.

The microscopic definition of $\mathbf{J}_\nu$ is simply

$$V\mathbf{J}_\nu = N_\nu m_\nu(\mathbf{u}_\nu - \mathbf{u}) , \tag{22}$$

where

$$N_\nu m_\nu \mathbf{u}_\nu = \sum_i{}^\nu \mathbf{p}_i , \tag{23}$$

$$(N_1 m_1 + N_2 m_2)\mathbf{u} = \sum_i \mathbf{p}_i . \tag{24}$$

However, it is more convenient for use in the NEMD "color-current" algorithm to define

$$V\mathbf{J}_D = N(\mathbf{u}_1 - \mathbf{u}_2) = N\left(\frac{1}{N_1 m_1} + \frac{1}{N_2 m_2}\right) V\mathbf{J}_1 . \tag{25}$$

Irving and Kirkwood[13] showed long ago that

$$V\mathbf{J}'_Q = \tfrac{1}{2}\sum_\nu \sum_i{}^\nu \left[\left(\frac{\mathbf{p}_i}{m_\nu} - \mathbf{u} \right) m_\nu \left(\frac{\mathbf{p}_i}{m_\nu} - \mathbf{u} \right)^2 + \sum_j \left(\frac{\mathbf{p}_i}{m_\nu} - \mathbf{u} \right) \cdot (\phi_{ij}\underline{\mathbf{1}} - \mathbf{q}_{ij}\mathbf{F}_{ij}) \right] . \tag{26}$$

As we have defined $\mathbf{J}_Q$ above to be that part of $\mathbf{J}'_Q$ excluding energy transport due to interdiffusion and we can equivalently state that $\mathbf{J}_Q$ must have no terms proportional to $\mathbf{u}_\nu - \mathbf{u}$, it is easy to see that

$$V\mathbf{J}_Q = \tfrac{1}{2}\sum_\nu \sum_i{}^\nu \left[\left(\frac{\mathbf{p}_i}{m_\nu} - \mathbf{u}_\nu \right) m_\nu \left(\frac{\mathbf{p}_i}{m_\nu} - \mathbf{u}_\nu \right)^2 + \sum_j \left(\frac{\mathbf{p}_i}{m_\nu} - \mathbf{u}_\nu \right) \cdot (\phi_{ij}\underline{\mathbf{1}} - \mathbf{q}_{ij}\mathbf{F}_{ij}) \right] . \tag{27}$$

We therefore find that

$$V(\mathbf{J}'_Q - \mathbf{J}_Q) = \sum_\nu (\mathbf{u}_\nu - \mathbf{u}) \cdot \left\{ \tfrac{1}{2}\sum_i{}^\nu \left[m_\nu \left(\frac{\mathbf{p}_i}{m_\nu} - \mathbf{u}_\nu \right)^2 + \sum_j \phi_{ij} \right] \underline{\mathbf{1}} + \sum_i{}^\nu \left[m_\nu \left(\frac{\mathbf{p}_i}{m_\nu} - \mathbf{u}_\nu \right) \left(\frac{\mathbf{p}_i}{m_\nu} - \mathbf{u}_\nu \right) - \tfrac{1}{2}\sum_j \mathbf{q}_{ij}\mathbf{F}_{ij} \right] + \tfrac{1}{2} N_\nu m_\nu (\mathbf{u}_\nu - \mathbf{u})^2 \underline{\mathbf{1}} \right\} . \tag{28}$$

Contact can be made with previous work by noting that (28) reduces to the result of Bearman and Kirkwood[14] [see also Ref. 11(b)] if we replace the tensor $E_\nu\underline{\mathbf{1}} + V\underline{P}_\nu$ by the (scalar) enthalpy of species ν, measured in the comoving frame of the species. Thus Bearman and Kirkwood's heat current definition is, apart from the last term in (28) which is negligible for linear response, a hybrid between the microscopic $\mathbf{J}'_Q$ of Irving and Kirkwood and the macroscopic equation (8). Whilst the Bearman-Kirkwood definition gives the correct heat current on a time-averaged basis (assuming that the off-diagonal elements of the pressure tensor have time average zero), (28) is clearly of more general validity and can be used as an instantaneous definition. The importance of this in the context of NEMD simulations will be remarked upon below.

It is convenient to define the tensors, for particle i of species ν,

$$\underline{S}_i = \frac{1}{2}\left[m_\nu \left(\frac{\mathbf{p}_i}{m_\nu} - \mathbf{u}_\nu \right)^2 \underline{\mathbf{1}} + \sum_k (\phi_{ik}\underline{\mathbf{1}} - \mathbf{q}_{ik}\mathbf{F}_{ik}) \right] ,$$
$$\underline{T}_i = \underline{S}_i - \frac{1}{N_\nu}\sum_j{}^\nu \underline{S}_j , \quad \sum_i{}^\nu \underline{T}_i = 0 . \tag{29}$$

Using these tensors we can now write

$$V\mathbf{J}_Q = \sum_\nu \sum_i{}^\nu \left(\frac{\mathbf{p}_i}{m_\nu} - \mathbf{u}_\nu \right) \cdot \underline{S}_i = \sum_\nu \sum_i{}^\nu \left(\frac{\mathbf{p}_i}{m_\nu} - \mathbf{u}_\nu \right) \cdot \underline{T}_i = \sum_\nu \sum_i{}^\nu \left(\frac{\mathbf{p}_i}{m_\nu} - \mathbf{u} \right) \cdot \underline{T}_i . \tag{30}$$

These expressions for the heat current are valid microscopically *and* instantaneously and therefore suitable for time averaging in simulations.

The phenomenological coefficients are related to the time-correlation functions of the microscopic currents through the Green-Kubo (GK) relations which, for an isotropic system, can be written as

$$L_{11}\underline{\mathbf{1}} = (V/k_B)\int_0^\infty dt \langle \mathbf{J}_1(t)\mathbf{J}_1(0)\rangle , \tag{31}$$

$$L_{1Q}\underline{\mathbf{1}} = (V/k_B)\int_0^\infty dt \langle \mathbf{J}_1(t)\mathbf{J}_Q(0)\rangle , \tag{32}$$

$$L_{QQ}\underline{\mathbf{1}} = (V/k_B)\int_0^\infty dt \langle \mathbf{J}_Q(t)\mathbf{J}_Q(0)\rangle . \tag{33}$$

A particularly clear general derivation is given by Zwanzig,[15] together with an explicit calculation for L_{11} which is easily modified to obtain L_{1Q} and L_{QQ}. Alternative methods of derivation are discussed in Zwanzig's review article.[16]

III. SIMULATIONS

A. NEMD algorithms

Morriss and Evans[17] have given the generalization of linear-response theory to a (one-component) system moving according to the (non-Hamiltonian) dynamics represented by the isokinetic equations of motion

$$\dot{\mathbf{q}}_i = \frac{\mathbf{p}_i}{m} + \underline{B}_i \cdot \mathbf{F}_{\text{ext}}(t) , \tag{34}$$

$$\dot{\mathbf{p}}_i = \mathbf{F}_i + \underline{C}_i \cdot \mathbf{F}_{\text{ext}}(t) - \alpha \mathbf{p}_i , \tag{35}$$

$$\alpha = \frac{\sum_i \mathbf{p}_i \cdot (\mathbf{F}_i + \underline{C}_i \cdot \mathbf{F}_{\text{ext}})}{\sum_i p_i^2} . \tag{36}$$

Here $\mathbf{F}_{\text{ext}}(t)$ is a constant force switched on at time $t=0$. Assuming that adiabatic incompressibility of phase space (AIΓ) (Ref. 1),

$$\sum_i \left[\frac{\partial}{\partial \mathbf{q}_i} \cdot \underline{B}_i + \frac{\partial}{\partial \mathbf{p}_i} \cdot \underline{C}_i \right] \cdot \mathbf{F}_{\text{ext}} = 0 , \tag{37}$$

is satisfied, then the linear response of any phase variable $\mathbf{J}_a$ with zero equilibrium average is given by

$$\lim_{t \to \infty} \langle \mathbf{J}_a(t) \rangle = (k_B T)^{-1} \int_0^\infty dt \langle \mathbf{J}_a(t) \dot{E}^{\text{ad}} \rangle , \tag{38}$$

where

$$\dot{E}^{\text{ad}} = \sum_i \left[\frac{\mathbf{p}_i}{m} \cdot \underline{C}_i - \mathbf{F}_i \cdot \underline{B}_i \right] \cdot \mathbf{F}_{\text{ext}} \tag{39}$$

is the adiabatic ($\alpha=0$) rate of energy dissipation due to the external force.

The idea of synthetic NEMD is to devise $\underline{B}_i$ and $\underline{C}_i$ so as to satisfy momentum conservation and AIΓ and such that $\dot{E}^{\text{ad}} = V \mathbf{J}_b \cdot \mathbf{F}_{\text{ext}}$ where $\mathbf{J}_b$ is one of the currents appearing in the GK relation for the required transport coefficient. By monitoring $\langle \mathbf{J}_a(t) \rangle$ for the resulting nonequilibrium steady state the GK expression can be evaluated from Eq. (38), leading to

$$\begin{aligned} L_{ab} &= \lim_{F_{\text{ext}} \to 0} M_{ab} , \\ M_{ab} &= T \lim_{t \to \infty} \frac{\langle J_a(t) \rangle}{F_{\text{ext}}} . \end{aligned} \tag{40}$$

Hitherto, NEMD simulations have been for pure fluids and the phase variable $\mathbf{J}_a$ in Eq. (38) has usually been the same current as the one appearing in $\dot{E}^{\text{ad}}$ since no L_{ab} with $a \neq b$ was expected to be nonzero. The only difference in the present work, apart from the thermostat (as discussed below) is that we expect both a heat current and a diffusion current to flow as a result of directly driving either one of them.

Because of the appearance of particle velocities relative to their species center of mass in the definition (27) of the heat current, it is convenient to introduce the following momentum variables:

$$\begin{aligned} p_\nu &= N_\nu^{-1} \sum\nolimits^\nu \mathbf{p}_i \cdot \hat{\mathbf{n}} , \\ \pi_i &= \mathbf{p}_i - p_\nu \hat{\mathbf{n}} \quad \text{for } i \text{ of species } \nu , \end{aligned} \tag{41}$$

where $\hat{\mathbf{n}}$ is a unit vector in the direction of $\mathbf{F}_{\text{ext}}$. We have anticipated with these definitions that the time-averaged currents generated will be in the same direction as the external force. We also introduce analogous force variables:

$$\begin{aligned} F_\nu &= N_\nu^{-1} \sum\nolimits^\nu \mathbf{F}_i \cdot \hat{\mathbf{n}} , \\ \mathbf{f}_i &= \mathbf{F}_i - F_\nu \hat{\mathbf{n}} \quad \text{for } i \text{ of species } \nu . \end{aligned} \tag{42}$$

With these definitions the system energy in the absence of external forces is

$$\begin{aligned} E &= E' + \sum_\nu N_\nu \frac{p_\nu^2}{2m_\nu} , \\ E' &= \sum_\nu \sum_i{}^\nu \frac{\pi_i^2}{2m_\nu} + \sum_i \sum_j \phi_{ij} . \end{aligned} \tag{43}$$

The equations of motion used for our thermal conductivity algorithm are analogous to the Evans algorithm[4] for pure substances:

$$\dot{\mathbf{q}}_i = \frac{1}{m_\nu} (\pi_i + p_\nu \hat{\mathbf{n}}) \quad \text{for } i \text{ of species } \nu , \tag{44}$$

$$\dot{p}_\nu = F_\nu , \tag{45}$$

$$\dot{\pi}_i = \mathbf{f}_i + \underline{T}_i \cdot \mathbf{F}_Q(t) - \alpha_Q \pi_i \quad \text{for } i \text{ of species } \nu , \tag{46}$$

$$\alpha_Q = \frac{\sum_\nu \frac{1}{m_\nu} \sum_i{}^\nu \pi_i \cdot (\mathbf{f}_i + \underline{T}_i \cdot \mathbf{F}_Q)}{\sum_\nu \frac{1}{m_\nu} \sum_i{}^\nu \pi_i^2} . \tag{47}$$

Here $\underline{T}_i$ is the tensor defined by Eq. (23), except that $\mathbf{p}_i - m_\nu \mathbf{u}_\nu$ is replaced by π_i, and so $\dot{E}^{\text{ad}} = V \mathbf{J}_Q \cdot \mathbf{F}_Q$. The mutual diffusion algorithm is a simple generalization of color self-diffusion:[3]

$$\dot{\mathbf{q}}_i = \frac{1}{m_\nu} (\pi_i + p_\nu \hat{\mathbf{n}}) \quad \text{for } i \text{ of species } \nu , \tag{48}$$

$$\dot{p}_\nu = F_\nu + c_\nu F_D(t) , \tag{49}$$

$$\dot{\pi}_i = \mathbf{f}_i - \alpha_D \pi_i , \tag{50}$$

$$\alpha_D = \frac{\sum_\nu \frac{1}{m_\nu} \sum_i{}^\nu \pi_i \cdot \mathbf{f}_i}{\sum_\nu \frac{1}{m_\nu} \sum_i{}^\nu \pi_i^2} . \tag{51}$$

Here $c_1 = N/N_1$ and $c_2 = -N/N_2$ so that $\dot{E}^{\text{ad}} = V \mathbf{J}_D \cdot \mathbf{F}_D$. It is easily shown that each of these algorithms satisfies AIΓ and momentum conservation.

Notice that the Gaussian thermostat multiplier (α_Q or α_D) is applied to π_i and *not* to $\mathbf{p}_i$. If it were applied to $\mathbf{p}_i$ and the simulation started away from the steady state, the thermostat would tend to prevent relaxation to the correct steady-state diffusion currents. This is related to the strictly correct definition of thermodynamic quantities for mixtures with interdiffusing species.[9] An alternative pro-

cedure[3] would be to thermostat only those momentum components perpendicular to the external force. Apart from their natural appearance in the kinetic part of the heat current, there is no particular advantage in using the peculiar variables p_ν and π_i. Noting that $\mathbf{u}=0$ in NEMD (the simulation cell may be regarded as a comoving fluid element in the Lagrangian hydrodynamic sense), it is easily seen from the last of Eqs. (30) that the thermal conductivity algorithm can equally well be formulated in terms of the usual momenta $\mathbf{p}_i$. Nevertheless, use of the peculiar variables makes it very obvious that the diffusion force $\mathbf{F}_D$ directly drives only the interspecies motion, whereas the thermal conductivity force $\mathbf{F}_Q$ directly drives only the intraspecies motion.

Although there is clearly some arbitrariness in the definition of the heat current, it is interesting to note that we were unable to devise a NEMD algorithm yielding $\dot{E}^{\text{ad}}=V\mathbf{J}_Q'\cdot\mathbf{F}_{\text{ext}}$ and also satisfying both momentum conservation and AIΓ.[1] It should be remarked, however, that these two conditions are not absolute necessities in NEMD: Gillan's thermal conductivity algorithm for pure substances[18] satisfies neither and yet is correct. The Evans algorithm is simpler to implement because of the noninstantaneous character of Gillan's equations of motion and heat current definition (similar to the Bearman-Kirkwood definition of heat current in mixtures).

B. Technical details

We studied an equimolar argon-krypton (denoted 1-2) mixture, modeled by Lennard-Jones (12-6) atoms with $m_1=39.95$ u, $m_2=83.80$ u, $\sigma_{11}=3.405$ Å, $\sigma_{22}=3.633$ Å, $\epsilon_{11}/k_B=119.8$ K, $\epsilon_{22}/k_B=167.0$ K, and σ_{12} and ϵ_{12} given by the Lorentz-Berthelot equations. The potential $\phi_{\nu\nu'}(q)$ was truncated at $q=2.5\sigma_{\nu\nu'}$ and raised to be continuous at the cutoff. All of our results are quoted, without special distinguishing notation, in reduced units defined with respect to the parameters m_1, σ_{11}, and ϵ_{11} appropriate to a pure argon fluid. The characteristic time is $\tau=\sigma_{11}\sqrt{(m_1/\epsilon_{11})}\approx 2$ ps. The temperature and density investigated were $k_BT/\epsilon_{11}=0.965$ and $N\sigma_{11}^3/V=0.7137$. This state point is precisely the one simulated by Jolly and Bearman[19] (JB) and is also one of those simulated by Jacucci and McDonald[20] (JM) and by Schoen and Hoheisel[21,22] (SH), all in connection with mutual diffusion.

Our simulations were all carried out on 108- or 256-particle systems with the usual periodic boundary conditions. The equations of motion were solved by a fourth order Gear predictor-corrector scheme. The slight discontinuities in the forces and their derivatives do not seem to cause any problems. Various methods were used to check the reliability of the computer programs and we briefly describe these. The programs were checked against the earlier NEMD results of Evans *et al.*[3] and Evans,[4] by using identical parameters for our two species. In the diffusion case, the algorithms are the same (apart from a factor 2 in the c_ν) and a single value of F_D is sufficient, but for the conductivity algorithm the present algorithm is only equivalent to the old one in the limit $F_Q\to 0$. (All these algorithms have no known physical meaning except in that limit.) Satisfactory agreement was found.

Internal consistency checks were also done: Using, instead of (47) and (51),

$$\alpha_Q=\frac{\sum_\nu \frac{1}{m_\nu}\left[\sum_i^\nu \boldsymbol{\pi}_i\cdot\underline{T}_i\cdot\mathbf{F}_Q-N_\nu p_\nu F_\nu\right]}{\sum_\nu \frac{1}{m_\nu}\sum_i^\nu \pi_i^2} \tag{52}$$

and

$$\alpha_D=-\frac{\sum_\nu N_\nu \frac{1}{m_\nu}p_\nu F_\nu}{\sum_\nu \frac{1}{m_\nu}\sum_i^\nu \pi_i^2}\,, \tag{53}$$

respectively, leads to $\dot{E}'=0$. A drift in E' of no more than 0.2% over 10^4 time steps was regarded as sufficiently small. This could be achieved with a time step of 0.005τ for $F_D\leqq 2.0$ or $F_Q\leqq 0.5$, but the time step had to be reduced to 0.003τ for $F_D=2.5$ and 0.0015τ for $F_Q=4.0$. (It is unreasonable to try to hold E constant when starting a run from a nonsteady state since then the enostat tends to prevent relaxation of the diffusion current.)

During our averaging runs, now with the thermostat equations (47) and (51), we corrected for slight temperature drift every 50 or 100 time steps. E is not a constant of the motion but, in the steady state, $\langle\dot{E}\rangle=0$. Hence we have

$$V\langle\mathbf{J}_D\rangle\cdot\mathbf{F}_D=N_dk_BT\langle\alpha_D\rangle\,, \tag{54}$$

$$V\langle\mathbf{J}_Q\rangle\cdot\mathbf{F}_Q=N_dk_BT\langle\alpha_Q\rangle\,, \tag{55}$$

where N_d is the number of degrees of freedom. In contrast to the common practice of making the approximation $N_d\approx 3N$, we use the exact value $N_d=3N-6$ appropriate to our algorithm. A legitimate question is whether this rare use of the correct temperature definition could be a significant factor in the comparison between our results and those of earlier workers, but this is precluded by the very large N used by SH.[21,22] Equations (54) and (55) were always satisfied well within statistical error for the averaging parts of our simulation runs and were also used as one indication of when a steady state had been achieved.

IV. RESULTS AND DISCUSSION

Tables I and II show the range of simulations carried out and give their lengths (in units of τ). The run lengths generally decrease quite sharply as the external force is increased from zero but some of the runs with low external forces were not continued long enough to get reasonable statistics for the cross coefficients and are therefore much shorter than would otherwise have been necessary. In addition, some of the runs with large external forces exhibited partial phase segregation which increased the required lengths, presumably due to fluctuations in the degree of phase segregation. The resultant fluxes due to the various

TABLE I. Thermal conduction simulations.

F_Q	Length (units of τ) $N=108$	$N=256$
0.10	2900	1225
0.15	7575	1450
0.20	1000	1000
0.25		300
0.30	900	225
0.40	800	1875
0.50	725	150
0.60	525	
0.80	3870	
1.00	175	
1.20	150	
1.50	105	
2.00	80	
2.50	135	
3.00	60	
3.50	150	
4.00	60	

external forces are given by Figs. 1–4. The errors indicated are standard errors calculated from 5000-time-step subaverages which are assumed to be approximately independent. This method of error estimation is quite crude and, if it were leading to serious underestimation, could undermine confidence in our results for the (small) cross coefficients. It is therefore reassuring that, using the same type of statistical analysis, in the test runs where the two species were made identical the cross currents were always consistent with zero, as they should be.

Figures 1 and 2 show graphs of M_{QQ} against F_Q and M_{11} against F_D, respectively. It can be seen that there is significant number dependence for large external forces. In the linear-response regime, however, only very slight number dependence can be detected within statistical errors in Fig. 1 and scarcely any at all in Fig. 2 (perhaps only because the statistical errors in Fig. 2 are rather larger). The extrapolated zero force values are estimated to be $L_{QQ}=3.95\pm0.05$ and $L_{11}=0.0145\pm0.0010$.

TABLE II. Mutual diffusion simulations.

F_D	Length (units of τ) $N=108$	$N=256$
0.10	4750[a]	825[a]
0.15	1000[a]	550[a]
0.25	275[a]	625[a]
0.50	1875	275[a]
0.75	3425	1050
1.00	875	525
1.25	630	1215
1.50	1275	
2.00	465	
2.25	240	
2.50	240[a]	

[a]Run of insufficient length to get reasonable statistics for cross coefficients.

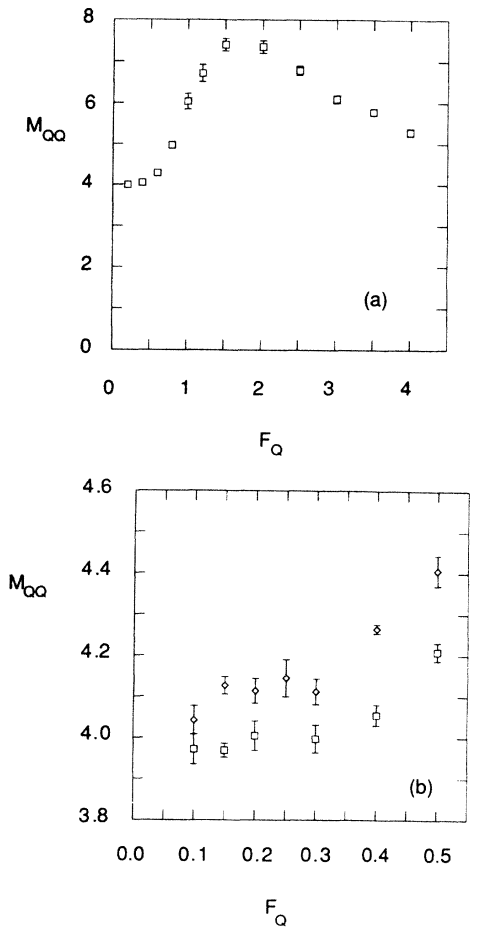

FIG. 1. Heat flows induced by the thermal conduction algorithm. Squares and diamonds represent 108- and 256-particle simulations, respectively. Error bars are not shown when they are smaller than the symbol height. (a) Large range of F_Q ($N=108$ only); (b) detail for small F_Q.

Only the latter value can be compared to those of other workers.[19–22] JB (Ref. 19) and SH (Ref. 22) have quoted values for D as defined by our equation (17). From these and their calculated values of the purely thermodynamic factor we can extract their values of L_{11}. We note that SH have clearly adopted the expression for D given by Eq. (1.14) of the JB paper although the first equation of Ref. 21 appears inconsistent with this by a multiplicative factor. Methods of obtaining the thermodynamic factor from the radial distribution functions are discussed in Refs. 19 and 21 but they do not lead to very accurate values and so we prefer to compare L_{11} directly. Admittedly we are here sidestepping a difficult problem which is of interest in its own right.

In the same reduced units as those we have used, the results of JM (Ref. 20), JB (Ref. 19), and SH (Ref. 22) are

$$(L_{11})_{\mathrm{JM}}=0.0170\ ,$$

$$(L_{11})_{\mathrm{JB}}=0.0165\ ,$$

$$(L_{11})_{\mathrm{SH}}=0.0174\ .$$

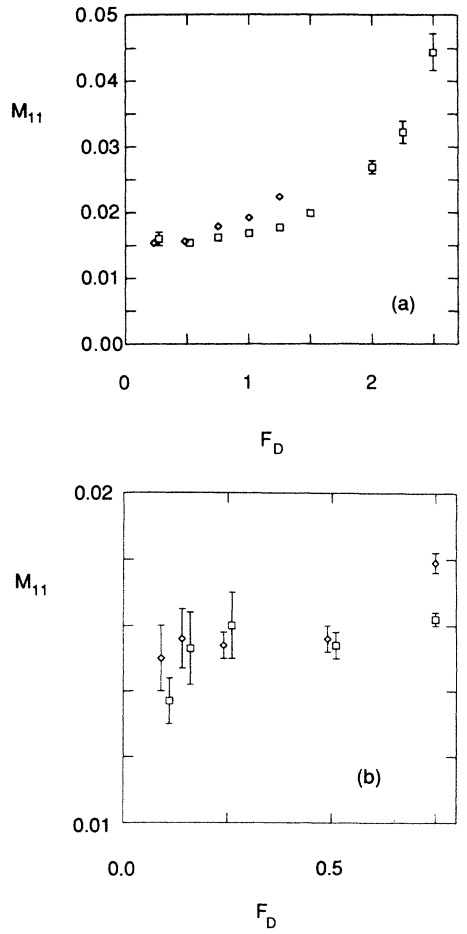

FIG. 2. Particle flows induced by the mutual diffusion algorithm. Symbols as in Fig. 1. (a) Large range of F_D; (b) detail for small F_D.

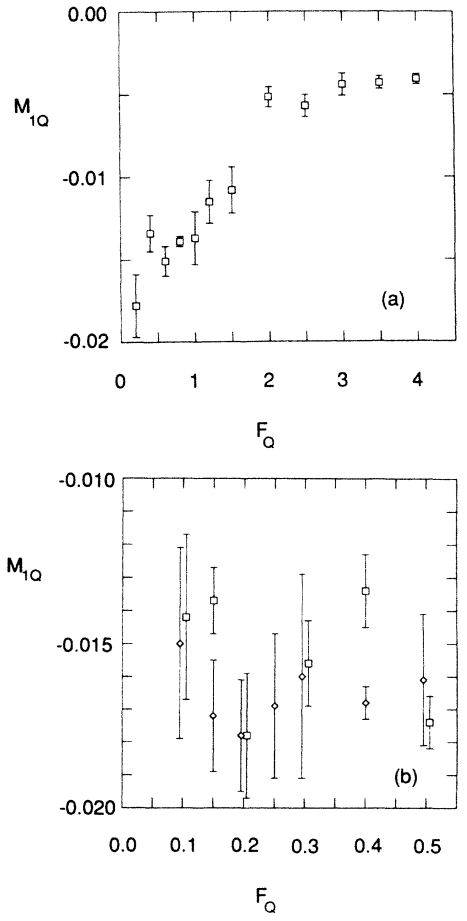

FIG. 3. Particle flows induced by the thermal conduction algorithm. Symbols as in Fig. 1. (a) Large range of F_Q ($N=108$ only); (b) detail for small F_Q.

Clearly the three results obtained from equilibrium simulations are nearly equal and the present NEMD result is $\sim 15\%$ lower. [The error of JB uncovered by SH (see Ref. 22) is in self-diffusion coefficients and should not invalidate the JB value of L_{11}.]

We cannot absolutely rule out the possibility of a sharp turning point in Fig. 2 which would lead to an underestimation of our value of L_{11}. With the computing resources available to us we cannot hope to get reasonable statistics for lower values of F_D. Nevertheless, we believe the NEMD result to be more reliable. An overestimate of L_{11} is just what is expected from truncated GK integration (or equivalently time differentiation of the rms displacement at finite time), since the negative tail of the relevant autocorrelation function is lost in noise and so, for dense liquid state points, a negative contribution to the GK integral is ignored. A warning against similar overestimation of the self-diffusion coefficient is found in the early work of Levesque and Verlet[23] and its existence was confirmed by Evans *et al.*[3] This effect may be much more dangerous when determining mutual diffusion coefficients for which much poorer statistics are obtained, despite the considerable effort made by SH in particular to overcome this problem. In particular, we stress that the careful investigation of number dependence by SH (Ref. 21) does *not* fully address this difficulty of the GK simulations. This could only be done, if at all, by a combination of a large system, high-precision arithmetic, *and* a high-precision finite-difference algorithm. In the absence of theory for the negative tail of the autocorrelation

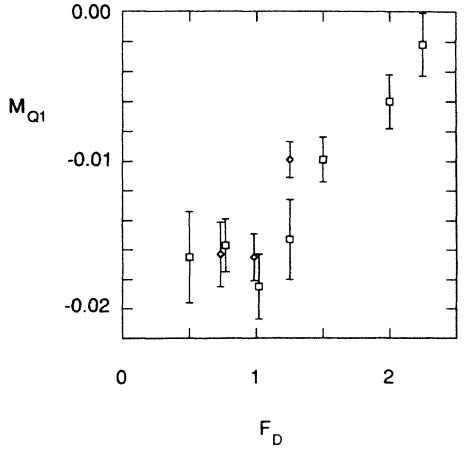

FIG. 4. Heat flows induced by the mutual diffusion algorithm. Symbols as in Fig. 1.

function, an informed extrapolation to $t=\infty$ is not possible.

Plots of M_{1Q} against F_Q and M_{Q1} against F_D are shown in Figs. 3 and 4, respectively. Any difference between 108- and 256-particle simulations is negligible within the statistical uncertainty, except for the single case $F_D=1.25$, but we expect that there would also be significant number dependence for the other high external forces where we only have 108-particle results. It will be noted that it is difficult to detect any definite trends for $F_Q<0.5$ or for $F_D<1.0$. This may indicate that, for the cross effects which are very weak, these forces are truly in the regime where linear response is valid so that no extrapolation is necessary. On the other hand, it may just be a consequence of larger statistical errors. Whichever of these explanations is correct, because of the lack of detectable force dependence we have estimated the zero-force extrapolated values from appropriately weighted averages of all values of M_{1Q} for $F_Q<0.5$ and all values of M_{Q1} for $F_D<1.0$. The results are, for $N=108$, $L_{1Q}=-0.0155\pm0.0005$ and $L_{Q1}=-0.0168\pm0.0013$, and for $N=256$, $L_{1Q}=-0.0168\pm0.0005$ and $L_{Q1}=-0.0164\pm0.0013$.

Evidently, L_{1Q} and L_{Q1} are equal within statistical error, which represents, to our knowledge, the first NEMD test of an ORR (though it is probably better regarded as yet another test of our NEMD algorithms). Based on the complete set of results, our final best estimate is $L_{1Q}=L_{Q1}=-0.0162\pm0.005$.

Before further discussing our results, we digress to describe their relation to experiments on real liquids. From Eqs. (20) and (21) and the values of heat current and thermal conductivity found in the simulations, it is easily deduced that the temperature gradient corresponding to $F_Q=0.1$ is $|\nabla T|\approx 3.5\times10^8$ K cm^{-1}. This is similar to the equivalent temperature gradients used by Evans[4] for pure liquid argon but many orders of magnitude greater than experimentally accessible values. Making a similar estimate of $|\nabla x_1|$ From Eqs. (15)–(17) is complicated by the purely thermodynamic factors. Taking the thermodynamic factor defined by JB and SH to be 1 and making the simplifying assumption that

$$v_2=\frac{V}{m_2}\frac{\sigma_2^3}{N_1\sigma_1^3+N_2\sigma_2^3}, \tag{56}$$

we find that $F_D=0.1$ corresponds to $|\nabla x_1|\approx 2\times10^6$ cm^{-1}. Since the maximum possible change of x_1 is 1, this value is clearly unrealistically high for a macroscopic fluid cell. As in all NEMD work, the gradient must be substantial on an atomic length scale to yield reasonable statistics.

With these same assumptions about the thermodynamic factors, we obtain from Eq. (19) the estimate $k_T=-0.28$. Thus for the minimum effective temperature gradient simulated ($|\nabla T|\approx 3.5\times10^8$ K cm^{-1}) the steady-state mass fraction gradient will be $|\nabla x_1|\approx 8\times10^5$ cm^{-1} For a more experimentally realistic temperature gradient of 10 K cm^{-1}, one would expect to find $|\nabla x_1|\approx 0.024$ cm^{-1}.

In order to obtain even such poor statistics for individual values of the cross currents, we have had to use much longer runs than are generally needed for pure fluids. As a by-product of these long runs, the accuracy of some of our values of M_{11} and especially M_{QQ} is rather better than has usually been obtained for pure fluids. Clearly, for a given length of run, better statistics are obtained from the conduction than from the diffusion algorithm. In part this reflects the nature of the physical processes involved: there is a sign change in the diffusion-current autocorrelation function but the heat-current autocorrelation function decays monotonically to zero. If we are only interested in obtaining $L_{1Q}=L_{Q1}$, then the thermal conductivity algorithm should be preferred. For the most straightforward comparison with experiment, however, k_T or some other coefficient closely related to L_{1Q}/L_{11} is required. This can only be obtained from the diffusion algorithm.

The poor statistics of the diffusion algorithm could be circumvented if extrapolation from higher values of F_D were possible. Unfortunately, there is a rapid increase in M_{11} above a system size-dependent value of F_D. We attribute this to a "finger instability" where the two species phase separate into counterstreaming fingers so that interspecies friction is significant only along a boundary or boundaries parallel to $\mathbf{F}_D$ and therefore greatly reduced from its value in a mixed phase. The phenomenon can be seen in typical instantaneous particle configurations projected on a plane perpendicular to $\mathbf{F}_D$. For $F_D=1.0$ the phase separation is only incipient, but it is quite fully developed for $F_D=2.5$. This phase separation at high F_D is an obstacle to the easy calculation of L_{11} and we are therefore investigating alternative diffusion algorithms where it may be suppressed. However, the chosen state point may be particularly hard to treat with our present diffusion algorithm since it is fairly close to the equilibrium phase separation.

Although it is a nuisance if we are only trying to determine L_{11}, this diffusively driven phase segregation is of interest in its own right and has already been studied in a closely analogous lattice model.[24,25] We plan a more detailed investigation using our continuum simulations but, apart from the evidence of particle configurations and the rapid increase of M_{11}, we can already easily see one other manifestation of the phase segregation in Fig. 4: at large F_D, $|M_{Q1}|$ decreases toward zero, an expected consequence of phase demixing since the Dufour effect is only found in mixtures. There is also some evidence of phase-transition behavior in the thermal conduction simulations at high F_Q but the exact nature of the change is not so clear.

V. CONCLUDING REMARKS

For the argon-krypton system studied, thermal diffusion is a small effect as expected, since the molecules are not very dissimilar. Even so, we have unambiguously detected both thermal diffusion and the Dufour effect. For an initially homogeneous (model) argon-krypton mixture in a thermal gradient, argon migrates toward higher temperatures. It is interesting to recall that, of the two phenomena, only thermal diffusion is easily found experimentally in liquids. The difficulty of measuring the

Dufour effect experimentally reflects, in addition to practical difficulties (principally lack of a suitable steady state), the greater statistical uncertainty found in the diffusion simulation.

To our knowledge, no cross coefficient has ever been obtained for a binary mixture by the GK equilibrium simulation method. We also believe the GK results for mutual diffusion in dense liquids to be unreliable because correlations over intervals longer than a few collision times are unobtainable due to noise in the simulations. (This problem still exists but is less important in the GK determination of thermal conductivities and viscosities.) In addition, since GK results are based on fluctuation formulas whereas NEMD results come from simple time averages, the former require longer runs to obtain similar statistics. Usually this is offset by the need to carry out the extrapolation to zero force in NEMD but such an extrapolation seems, on the basis of our calculation here, to be less important in obtaining L_{1Q} ($=L_{Q1}$). Our NEMD algorithms therefore seem well suited to the task of making a systematic study of thermal diffusion.

Probably the best available theory of transport coefficients in a dense fluid mixture is the revised Enskog theory (RET).[26] It is directly applicable only to hard-sphere (HS) mixtures but could be modified in a straightforward way to handle continuous potentials as was done for pure fluids.[27] The published RET results for binary HS mixtures[28] only give mutual diffusion coefficients and the mass ratios studied are all much higher than in our simulation. We therefore attempt no comparison of our results with RET. Even for more similar mixtures, such a comparison would not be particularly illuminating since we have only simulated a single-state point while the main question about RET is whether it correctly predicts trends. We hope to carry out a more extensive set of NEMD simulations for HS mixtures. This will provide a more direct test of RET itself because the extra step of finding effective HS diameters for continuous potentials will be eliminated.

Note added in proof. After this work had been completed, it was pointed out to us by Professor R. J. Bearman that, contrary to the impression given above, there has been an accurate experimental measurement of the Dufour effect in liquids.[29]

ACKNOWLEDGMENTS

D.M. would like to thank Gary Morriss for advice on computing. D.J.E. thanks Dennis Isbister for assistance in the early stages of this work.

APPENDIX

In the definition of $\nabla_T \mu_\nu$ appearing in Eq. (9), we have deliberately left the meaning of $\partial\mu_\nu/\partial T$ somewhat imprecise. In the usual application of the macroscopic formalism (to experiments) the exact meaning intended is $(\partial\mu_\nu/\partial T)_{p,\{N\}}$. Correspondingly, h_ν in Eq. (8) is interpreted as

$$h_\nu = \frac{1}{m_\nu}\left[\frac{\partial H}{\partial N_\nu}\right]_{T,p,\{N\}'} = \mu_\nu - T\left[\frac{\partial \mu_\nu}{\partial T}\right]_{p,\{N\}}, \quad \text{(A1)}$$

where H is the total enthalpy. $\{N\}$ represents the complete set of numbers of particles of all species and $\{N\}'$ is $\{N\}$ with N_ν omitted. The microscopic formalism would be consistent with this if the ensemble averages in Eqs. (31)–(33) and (40) were in the $(T,p,\{N\})$ ensemble but in the NEMD simulations the ensemble is $(T,v,\{N\})$ where v represents the volume per particle.

Therefore, in the context of NEMD simulations, we strictly ought to make the interpretation

$$h_\nu = \frac{1}{m_\nu}\left[\frac{\partial H}{\partial N_\nu}\right]_{T,v,\{N\}'} = \mu_\nu - T\left[\frac{\partial \mu_\nu}{\partial T}\right]_{v,\{N\}} - \left[\frac{\partial \mu_\nu}{\partial v}\right]_{T,\{N\}} \quad \text{(A2)}$$

and correspondingly replace $\nabla_T \mu_\nu$ by

$$\nabla_{T,v}\mu_\nu = \nabla\mu_\nu - \left[\frac{\partial \mu_\nu}{\partial T}\right]_{v,\{N\}}\nabla T - \left[\frac{\partial \mu_\nu}{\partial v}\right]_{T,\{N\}}\nabla v\,. \quad \text{(A3)}$$

That is, we remove from the chemical potential gradient those parts caused by gradients in both temperature and total number density. The extra terms in (A2) and (A3) lead to a small ensemble correction between the simulation and experimental results. In the particular argon-krypton mixture studied the correction will be negligible because the mixture is very close to ideal.[19,21]

*Permanent address: BP Research Centre, Chertsey Road, Sunbury-on-Thames, Middlesex TW16 7LN, United Kingdom.

[1] D. J. Evans and G. P. Morriss, Comput. Phys. Rep. 1, 297 (1984).

[2] A. W. Lees and S. F. Edwards, J. Phys. C 5, 1921 (1972).

[3] D. J. Evans, W. G. Hoover, B. H. Failor, B. Moran, and A. J. C. Ladd, Phys. Rev. A 28, 1016 (1983).

[4] D. J. Evans, Phys. Lett. A 91, 457 (1982).

[5] C. Massobrio and G. Ciccotti, Phys. Rev. A 30, 3191 (1984).

[6] W. G. Hoover, B. Moran, and J. M. Haile, J. Stat. Phys. 37, 109 (1984).

[7] D. J. Evans, Phys. Rev. A 34, 1449 (1986).

[8] M. J. Gillan and R. W. Holloway (unpublished).

[9] S. R. deGroot and P. Mazur, *Nonequilibrium Thermodynamics* (Dover, New York, 1984).

[10] D. D. Fitts, *Nonequilibrium Thermodynamics* (McGraw-Hill, New York, 1962).

[11] (a) H. J. M. Hanley, in *Transport Phenomena in Fluids,* edited by H. J. M. Hanley (Dekker, New York, 1969), Chaps. 1–3; (b) W. A. Steele, *ibid.*, Chap. 8.

[12] C. S. Hartley and J. Crank, Trans. Faraday Soc. 45, 801 (1949).

[13] J. H. Irving and J. G. Kirkwood, J. Chem. Phys. 18, 817 (1950).

[14] R. J. Bearman and J. G. Kirkwood, J. Chem. Phys. 28, 136

(1958).
[15]R. Zwanzig, J. Chem. Phys. **40**, 2527 (1964).
[16]R. Zwanzig, Annu. Rev. Phys. Chem. **16**, 67 (1965).
[17]G. P. Morriss and D. J. Evans, Mol. Phys. **54**, 629 (1985).
[18]M. J. Gillan and M. Dixon, J. Phys. C **16**, 869 (1983).
[19]D. L. Jolly and R. J. Bearman, Mol. Phys. **41**, 137 (1980).
[20]G. Jacucci and I. R. McDonald, Physica A **80**, 607 (1975).
[21]M. Schoen and C. Hoheisel, Mol. Phys. **52**, 33 (1984).
[22]M. Schoen and C. Hoheisel, Mol. Phys. **52**, 1029 (1984).
[23]D. Levesque and L. Verlet, Phys. Rev. A **2**, 2514 (1970).
[24]S. Katz, J. L. Lebowitz, and H. Spohn, J. Stat. Phys. **34**, 497 (1984).
[25]J. Marro, J. L. Lebowitz, H. Spohn, and M. H. Kalos, J. Stat. Phys. **38**, 725 (1985).
[26]M. Lopez de Haro, E. G. D. Cohen, and J. M. Kincaid, J. Chem. Phys. **78**, 2746 (1983).
[27]J. V. Sengers, Int. J. Heat Mass Transfer **8**, 1103 (1965).
[28]J. M. Kincaid, M. Lopez de Haro, and E. G. D. Cohen, J. Chem. Phys. **79**, 4509 (1983).
[29]R. L. Rowley and F. H. Horne, J. Chem. Phys. **68**, 325 (1978); **72**, 131 (1980).